Energy and AI 16 (2024) 100371

Contents lists available at ScienceDirect

Energy and AI

journal homepage: www.sciencedirect.com/journal/energy-and-ai

# Forecasting solar power generation using evolutionary mating algorithm-deep neural networks

Mohd Herwan Sulaiman [a,*], Zuriani Mustaffa [b]

[a] Faculty of Electrical & Electronics Engineering Technology, Universiti Malaysia Pahang Al-Sultan Abdullah (UMPSA), 26600 Pekan Pahang, Malaysia
[b] Faculty of Computing, Universiti Malaysia Pahang Al-Sultan Abdullah (UMPSA), 26600 Pekan Pahang, Malaysia

## HIGHLIGHTS

- Evolutionary mating algorithm used in optimizing deep neural networks for PV output forecasting.
- Real data from solar power plant measurements spanning a 34-day period is utilized.
- EMA-DNN shows potential in forecasting the PV AC power output.

## GRAPHICAL ABSTRACT

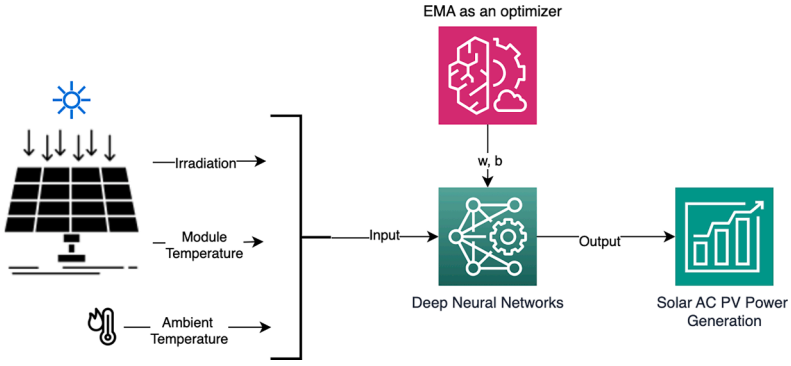


## ARTICLE INFO

*KEYWORDS:*
Deep learning neural networks
Evolutionary mating algorithm
Feed forward neural networks
Metaheuristic Optimizers
Solar PV

## ABSTRACT

This paper proposes an integration of recent metaheuristic algorithm namely Evolutionary Mating Algorithm (EMA) in optimizing the weights and biases of deep neural networks (DNN) for forecasting the solar power generation. The study employs a Feed Forward Neural Network (FFNN) to forecast AC power output using real solar power plant measurements spanning a 34-day period, recorded at 15-minute intervals. The intricate nonlinear relationship between solar irradiation, ambient temperature, and module temperature is captured for accurate prediction. Additionally, the paper conducts a comprehensive comparison with established algorithms, including Differential Evolution (DE-DNN), Barnacles Mating Optimizer (BMO-DNN), Particle Swarm Optimization (PSO-DNN), Harmony Search Algorithm (HSA-DNN), DNN with Adaptive Moment Estimation optimizer (ADAM) and Nonlinear AutoRegressive with eXogenous inputs (NARX). The experimental results distinctly highlight the exceptional performance of EMA-DNN by attaining the lowest Root Mean Squared Error (RMSE) during testing. This contribution not only advances solar power forecasting methodologies but also underscores the potential of merging metaheuristic algorithms with contemporary neural networks for improved accuracy and reliability.

* Corresponding author.
*E-mail address:* herwan@ump.edu.my (M.H. Sulaiman).

https://doi.org/10.1016/j.egyai.2024.100371

Available online 17 April 2024

## 1. Introduction

Renewable energy sources, such as solar power, play a pivotal role in addressing the challenges of energy sustainability and climate change mitigation [1,2]. Accurately forecasting photovoltaic (PV) AC power generation is crucial for effectively managing power grids, seamlessly incorporating renewable energy sources, and making informed decisions. However, achieving high forecasting accuracy remains challenging due to the inherent variability and uncertainty associated with solar power generation. Several factors contribute to this complexity. The non-linear relationships between key variables such as solar irradiation, ambient temperature, and module temperature significantly impact power output [3]. In addition, the effect of environmental variables on the efficiency of solar PV plants in determining the optimal sites of solar plant also play a vital role for increasing the efficiency [4]. Apart of that, weather variability, including cloud cover and rapid changes in irradiance, can introduce significant forecasting errors. Furthermore, partial shading, caused by factors like nearby objects or uneven cleaning, can lead to localized reductions in power output that are often difficult to predict using traditional forecasting methods [5,6].

Recognizing these challenges, the need for deep learning in PV forecasting is paramount due to its ability to handle complex patterns and relationships in the data, improving forecast accuracy [7]. Additionally, deep learning-based forecasting systems can provide real-time forecasts, crucial for managing power systems with high PV generation penetration. Integration of deep learning with optimization algorithms is necessary to further improve the performance of photovoltaic power forecasting models. Optimization algorithms can help in finding the optimal values for the parameters of deep learning models, leading to better prediction accuracy [8,9]. As the study unfolds, the focus is on elucidating how this integration addresses the complexities of solar power forecasting, ultimately contributing to enhanced efficiency and reliability. To this end, the integration of advanced optimization algorithms with deep learning techniques has gained prominence in enhancing prediction accuracy [10–19].

In recent years, the synergy between metaheuristic optimization algorithms and deep learning has garnered significant attention in various domains [20–30], with a growing focus on their application in renewable energy prediction [18,31–33], particularly for solar power forecasting. Metaheuristic algorithms draw inspiration from natural processes to explore solution spaces efficiently and tackle complex optimization problems [34–40]. Various algorithms have emerged as a promising contender due to its efficacy in solving diverse optimization tasks. Generally, metaheuristic algorithms can be categorized into four groups: evolution-based, physics-based, swarm-based and human-based algorithms [41]. Inspired by nature and natural phenomena such as reproduction, survival, and the Earth's gravity, these algorithms leverage different principles. Evolutionary algorithms, belonging to the first category, emulate genetic processes like crossover, mutation, and reproduction [42]. Physics-based algorithms, the second category, draw inspiration from physical phenomena in nature. For instance, the Gravitational Search Algorithm (GSA) models the interaction between masses based on Newtonian physics [43]. The third category comprises swarm intelligence algorithms, or swarm-based algorithms, which derive inspiration from the behaviors of animals in nature. Examples include the particle swarm optimization algorithm (PSO), which mimics the movement of particles [44] and has been employed to optimize the tilt angle of solar panels to maximize power generation [45]. Finally, the human-based algorithms mimics the human interaction or activities in finding the optimization solution such as Teaching-Learning based optimization (TLBO) [46], Harmony Search Algorithm (HSA) [47] and many more.

Deep Neural Networks (DNNs), on the other hand, have demonstrated remarkable capabilities in capturing intricate relationships in data [48], including those present in historical data [49,50]. DNNs consist of interconnected layers of neurons that transform input data into desired output through weighted connections and activation functions which normally utilized for regression and classification problems [51–59]. The application of DNNs in solar power generation forecasting has showcased their potential in modeling complex non-linear relationships [60–64]. However, their performance greatly hinges on the quality of weights and biases. These values determine the strength of connections between neurons and influence how the network processes information. Finding the optimal weights and biases is crucial for maximizing DNN accuracy [65]. Nonetheless, the integration of these methodologies for accurate solar power generation prediction remains an area that has not yet been extensively explored, and there is still a need for further investigation and advancements.

The knowledge gap lies in the comprehensive integration of these emerging paradigms to address the intricate nature of solar power generation prediction. Current hybrid approaches often focus on single-aspect optimization or lack the adaptability to handle the dynamic complexities of solar power data [11]. To address this gap, this study introduces a pioneering hybrid approach called Evolutionary Mating Algorithm [66]-Deep Neural Networks(EMA-DNN) for precise PV AC power generation forecasting. The EMA algorithm offers advantages in [65,67] in terms of efficient exploration of the search space over other metaheuristic algorithms. By harnessing the synergies between EMA and DNNs, this study aims to transform accurate prediction techniques by merging optimization capabilities with deep learning capacity.

By conducting meticulous experiments and comprehensive evaluations, the efficacy of the proposed approach is systematically determined in contrast to other contemporary metaheuristic-DNN models. The paper employs a Feed Forward Neural Network (FFNN) to forecast PV AC power generation in solar plants based on a 34-day dataset of real measurements [68]. The research not only delves into the effectiveness of the recent EMA algorithm but also conducts a comparative analysis with other well-established metaheuristic algorithms, including Differential Evolution (DE) [69], Barnacles Mating Optimizer (BMO) [41], Particle Swarm Optimization (PSO) [44], and Harmony Search Algorithm (HSA) [47].

This study endeavors to contribute substantively to the body of knowledge in machine learning, optimization, and solar energy forecasting, fostering innovative methodologies that could reshape accurate PV AC power generation prediction. The selection of appropriate optimization algorithms for training DNNs in the context of solar energy prediction is crucial for effective model development. While gradient-based methods, such as stochastic gradient descent (SGD) and Adaptive Moment Estimation (ADAM), are widely employed, this study deliberately investigated the potential of non-gradient optimization algorithms, specifically focusing on metaheuristic approaches. This decision was motivated by the inherent limitations associated with gradient-based techniques. These methods can become trapped in local optima, hindering their ability to explore the entire solution space and potentially leading to suboptimal outcomes [34].

Furthermore, the No-Free-Lunch (NFL) theorem, a fundamental principle in optimization theory, posits that no single optimization algorithm can consistently outperform all others across all problem domains. By embracing metaheuristic optimization algorithms, this study aligns with the spirit of the NFL theorem, acknowledging that the effectiveness of an optimization method is contingent upon the specific problem characteristics [36]. In summary, the contribution of this research study can be summarized as follows:

- Bridging optimization and deep learning for solar power prediction.
- Pioneering the EMA-DNN hybrid approach.
- Filling the gap in accurate solar power generation prediction.
- Advancing machine learning, optimization, and solar energy forecasting domains.

The rest of the paper is organized as follows: Section 2 discusses the data analysis followed by brief information about EMA in Section 3.

Section 4 presents the DNN model and the application of EMA in optimizing the weights and biases of DNN is presented in Section 5. Results and discussion are presented in Section 6 and finally, Section 7 states the conclusion of the paper.

## 2. Data analysis

The dataset utilized in this study originates from two solar power plants situated in India, spanning a comprehensive time frame of 34 days, specifically from 15 May 2020 12AM until 17 June 2020 11.45PM, with measurements captured at 15-minute intervals [68]. The dataset encompasses weather-related data, sourced from a singular sensor at the plant level, which encapsulates ambient conditions. Concurrently, power generation data is acquired from numerous individual inverters dispersed across the solar plants. In this paper, a meticulous focus is directed toward the data originating exclusively from Plant 1. This selective inclusion ensures a refined and contextually relevant exploration of the solar power generation dynamics, enriched by a specific geographical and operational context.

The dataset comprises 22 inverters, encompassing variables like daily yield, total yield, as well as AC and DC power outputs. Notably, the dataset is marked by certain gaps, evident from the recorded count of 3158 data points, a contrast to the anticipated 3264 unique timestamps at the plant level (calculated based on a 34-day span, with 24 h, each containing 4 (15-minute intervals)). This dataset also encompasses crucial weather sensor measurements, namely irradiation, ambient temperature, and module temperature. Following a meticulous data cleaning process, a streamlined approach is adopted wherein unmatched data is pruned. Ultimately, 3158 instances remain for analysis in this study.

The data cleaning process encompasses a thorough examination and processing of outliers and missing data. In addressing missing datetimes within the generation and weather sensor datasets, a datetime object is crafted, covering the entire range of expected datetimes. Given variations in missing datetimes across different inverters, this process is meticulously executed for each inverter individually, followed by concatenation to reconstruct the complete dataset. To delve deeper into the dataset's characteristics, a comprehensive analysis involves extracting basic datetime features. While considering the modeling potential throughout the year and month could account for seasonal variations and long-term trends, it is judiciously omitted due to the dataset's limited coverage of 34 days.

Regarding outliers, a rigorous examination is undertaken, starting with a quick check for any negative power values, all of which were found to be non-existent. Specifically targeting outliers, instances where midday power generation records as zero prompt a detailed investigation. This phenomenon could stem from various factors such as bad data, malfunctioning inverters, planned maintenance, or environmental conditions like cloudy or sunny days. The observed occurrences, notably on Sundays, may indicate scheduled maintenance, given the likelihood of lower grid demand on that day. The data cleaning process concludes with the imputation of missing values through interpolation and concatenation, serving as a final step before initiating the modeling phase. These steps collectively contribute to a robust and refined dataset for subsequent analysis and forecasting.

To configure the input-output framework, a meticulous assessment of linear correlations is conducted. The correlation heatmap, depicted in Fig. 1, provides a graphical insight into these vital relationships within the dataset.

From Fig. 1, it can be seen that a distinct correlation between DC and AC power becomes apparent, signifying the proficient operation of inverters in converting DC to AC power. As a result, this paper focuses on utilizing AC POWER as the target variable. An equally robust correlation emerges between HOUR and DAILY YIELD, aligning with the intuitive notion of daily yield progressively increasing throughout the day. Pertaining to the weather sensor data, noteworthy correlations emerge between IRRADIATION and AC POWER, as well as between MODULE TEMPERATURE and AC POWER [70]. These correlations resonate with established findings, underscoring the influential role of irradiation, ambient conditions, and module temperature in photovoltaic power

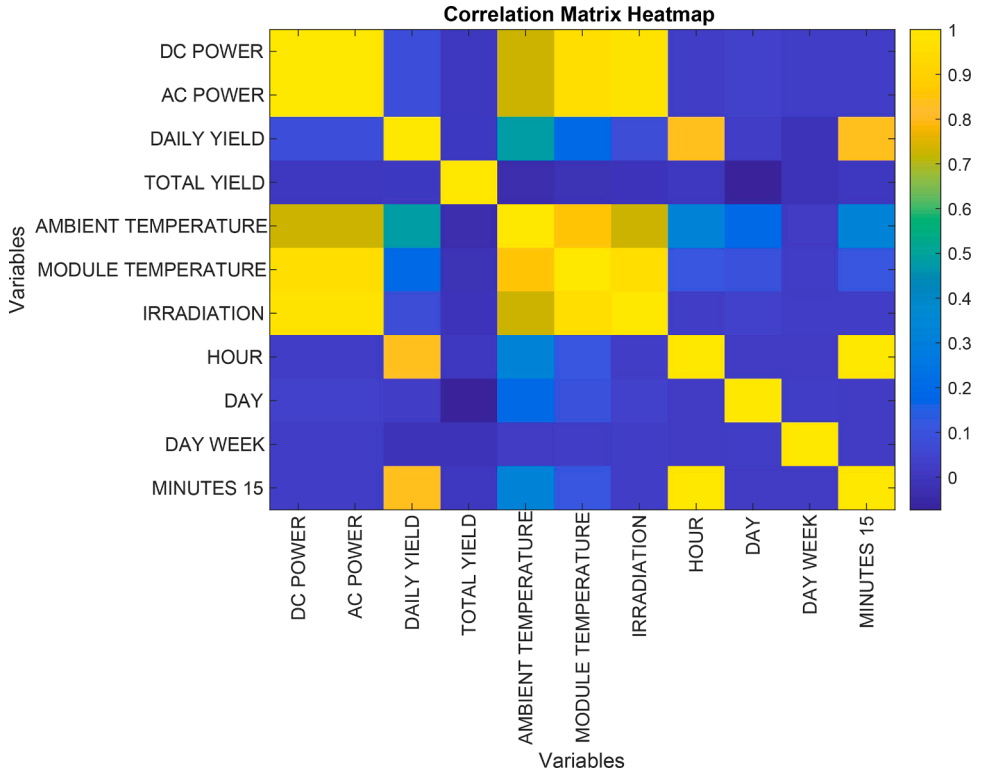


**Fig. 1.** Heatmap for linear correlation of the features.

generation [63,71]. Guided by these significant correlations and supported by relevant literature, the input-output configuration for this study is judiciously selected, comprising irradiation, ambient and module temperature data as input variables, with AC power as the target variable. This integrated approach bolsters the robustness and credibility of the variable selection for the solar power forecasting model.

Fig. 2 illustrates the focal point of the study, which is the AC power generation over a week from June 10th to June 17th, 2020. The data depicts the cumulative power output aggregated from 22 individual inverters. Evidently, the visual representation unveils the presence of frequent valleys and distinct peaks, signifying dynamic variations in the power generation profile. The presence of valleys in the AC power generation data can be attributed to factors such as low solar intensity during cloudy periods, causing temporary decreases in power output. Additionally, sharp peaks are likely a result of optimal conditions, including high solar irradiance on clear days, leading to intensified power generation. These fluctuations could also be influenced by the behavior of the solar inverters, which convert DC power from panels to AC power.

In order to provide a deeper understanding of the observed trend, an investigation was conducted specifically on the power outputs of a single inverter, identified as inverter #5. This focused analysis, as illustrated in Fig. 3, highlights the intricacies of power generation patterns associated with a singular unit. The exploration aimed to uncover any underlying factors that might contribute to the phenomenon of valleys and sharp peaks witnessed in the broader AC power generation data. By isolating the behavior of a single inverter, a more detailed perspective was gained, offering insights into how operational dynamics and environmental variables might influence the distinct variations in power output over time.

## 3. Evolutionary mating algorithm

Evolutionary Mating Algorithm (EMA) [66], a novel metaheuristic algorithm inspired by biological mating mechanisms, draws its foundations from the principles of Hardy-Weinberg (HW) [72]. Much like its metaheuristic counterparts, EMA encompasses three core phases: initialization, selection, and offspring generation. The initialization step segregates the candidate solution $X$ into distinct groups: one comprising male denoted as $X_m$ and the other composed of females represented by $X_f$. This partitioning process can be succinctly expressed as follows:

$$X_m = \begin{bmatrix} x_1^1 & \cdots & x_1^d \\ \vdots & \ddots & \vdots \\ x_{n/2}^1 & \cdots & x_{n/2}^d \end{bmatrix} \tag{1}$$

$$X_f = \begin{bmatrix} x_{\frac{n}{2}+1}^1 & \cdots & x_{\frac{n}{2}+1}^d \\ \vdots & \ddots & \vdots \\ x_n^1 & \cdots & x_n^d \end{bmatrix} \tag{2}$$

In this context, the symbol $d$ signifies the dimension of the problem, while $n$ denotes the size of the population. Following the initialization phase, every member of the population undergoes fitness function evaluation, and the optimal solutions are identified and documented from both $X_m$ and $X_f$. The mating mechanism in EMA draws inspiration from the concept of sexual selection, designated as $I_{mates}$, which can be succinctly represented as follows:

$$I_{mates} = 1 + \left[ var\left(X_{m,*}^T\right) - var\left(X_{f,*}^T\right) \right] \tag{3}$$

where $var(X_m^T)$ and $var(X_f^T)$ represent the variance of the selected male and female to be mated, respectively, at iteration $T$. To produce new offspring, $X_{child}^T$, the following equation is used:

$$X_{child}^T = \begin{cases} p. * X_{m,*}^T + q. * x_{f,*}^T & for \quad I_{mates} \geq 0 \\ p. * X_{f,*}^T + q. * x_{m,*}^T & for \quad I_{mates} < 0 \end{cases} \tag{4}$$

where $p$ denotes a normally distributed random variable expressed as $p$

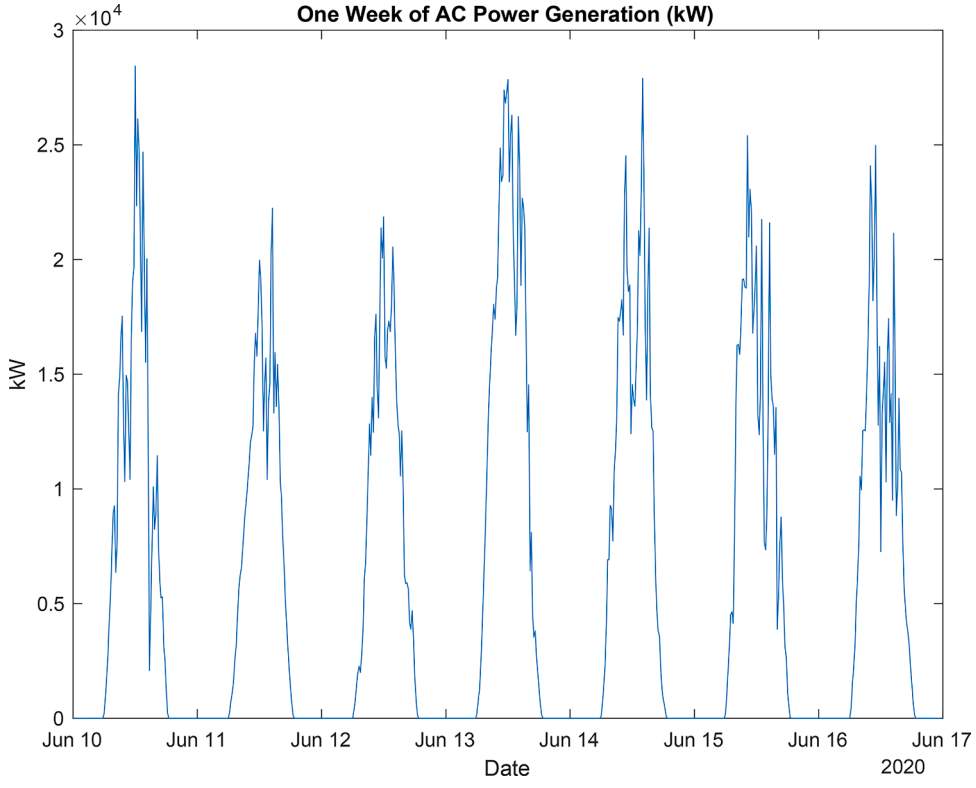


**Fig. 2.** AC power generation for one week.

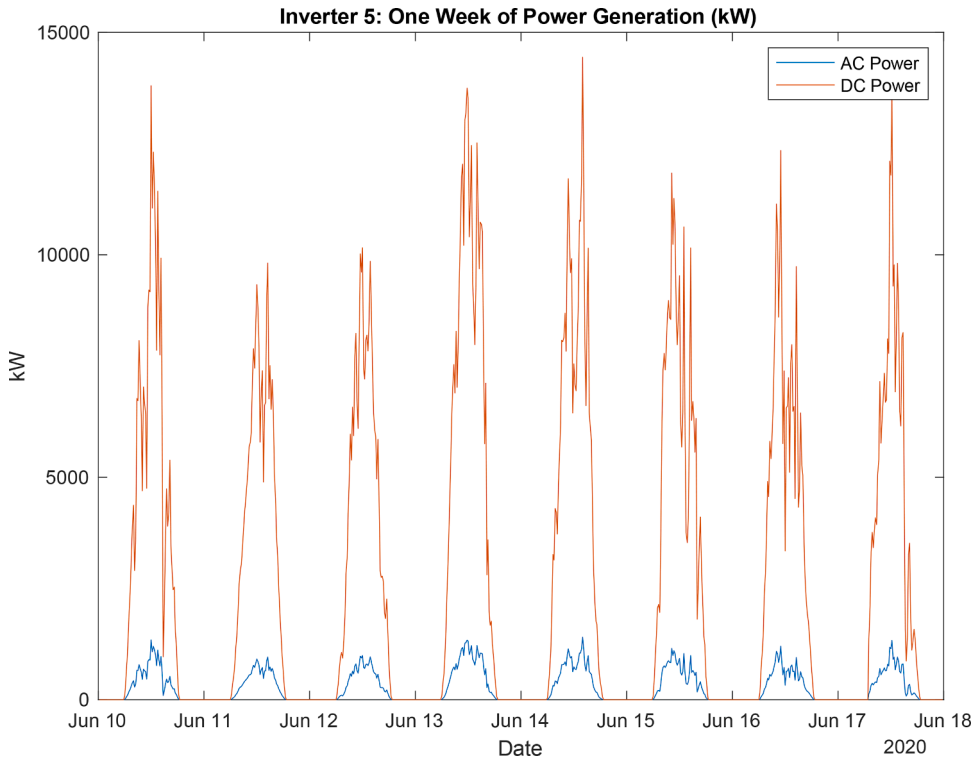


**Fig. 3.** AC and DC power generation for one week for inverter #5.

$= randn\,(1, d)$, while $q$ is defined as the complementary value to $p$, i.e., $q = (1 - p)$. Within the framework of EMA, the algorithm accommodates the influence of environmental factors, akin to encountering a predator, which is treated as a form of exploratory activity. This exerted influence significantly shapes the characteristics of the optimal solution, contingent upon whether the offspring survives or does not. The dimensions of newly generated solutions (offspring) can be further influenced by both the best solution identified initially and the best solutions found during each iteration, as followed:

$$X_{child}^{T+1} = K. * X_{child,j}^{T} + X_{j}^{best}. * (1 - K) j = 1, 2, \ldots d \tag{5}$$

where $X_j^{best}$ is the current best solution at a particular iteration and $K$ can be obtained from the following expression:

$$K = rand(1, d) < Cr \tag{6}$$

where $Cr$ is the pre-set value of crossover probability. As been mentioned, the likelihood of encountering the "predator" (denoted by $r$) needs to be adjusted based on the specific optimization problem being tackled. During each iteration, the following steps encourage exploration:

$$X_{child}^{T+1} = rand(1, d). * X_{j}^{best} \quad for \quad r <\in [0, 1] \tag{7}$$

The parameters $Cr$ and $r$ necessitate calibration, representing the predetermined values for crossover probability and the likelihood of encountering the predator, respectively. Further comprehensive insights regarding EMA are available in [66].

## 4. Deep learning feed-forward neural networks model

The forecast of AC power output is achieved by fine-tuning the weights and biases of a deep learning neural network (DNN) using the Evolutionary Mating Algorithm (EMA). This DNN takes into account input variables like irradiation, ambient and module temperatures, and

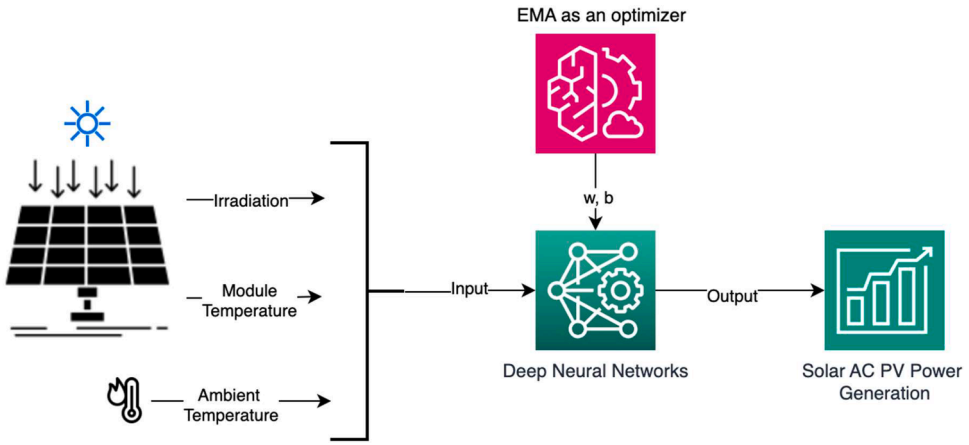


**Fig. 4.** Proposed EMA-DNN for forecasting the PV AC power output.

predicts the PV AC power output in kilowatts. Fig. 4 provides an overview of the proposed method for predicting solar AC power generation in the solar power plant. It outlines the flow of the process and highlights the connection between input-output data configuration as well as EMA is utilized as an optimizer for weights and biases optimization of DNN for forecasting the PV AC power generation.

It is important to note that the collected data serves as the foundation for the model's learning process. Generally, as the amount of data increases, the DNN has a greater chance of learning the complex relationships between the input and output variables, potentially leading to improved accuracy in solar power generation prediction. This observation aligns with the findings reported in [73]. The dataset utilized for both training and evaluating the forecasting model encompasses a span of 34 days, each featuring distinct input-output configurations. This dataset is partitioned into three sets: a training set comprising 21 days, a validation set spanning 10 days, and a final 3-day period dedicated to testing the model's performance. These divisions are visually depicted in Figs. 5 and 6, providing a clear representation of the data distribution across the different phases of model development and assessment.

## 5. EMA FOR optimizing the weigths and biases of DNN

The deep neural network (DNN) architecture employed in this study comprises two hidden layers within a feed forward neural network, as depicted in Fig. 7. The input layer encompasses three inputs: irradiation, ambient temperature, and module temperature, measured at the inverter. These inputs function as the DNN's input features. Each hidden layer is configured with five neurons, while the output layer incorporates a single neuron that signifies the forecasted PV AC power output. The activation functions employed in the DNN for each layer are defined as follows:

$$\text{Input layer}: \text{ linear function } y = u \tag{8}$$

$$\text{Hidden layer 1}: \text{ hyperbolic tangent } y = \frac{e^{u} - e^{-u}}{e^{u} + e^{-u}} \tag{9}$$

$$\text{Hidden layers 2}: \text{ leaky rectified linear unit } ReLU\ y = max(0.3 \times u, u) \tag{10}$$

$$\text{Output layer}: \text{ clipped } ReLU\ y = min[max(0, u), 1] \tag{11}$$

Within each neuron, the output ($y$) is established through the summation of the total input ($u$) accumulated prior to entering the neuron. This total input is computed by adding up the products of the inputs ($x_i$) with their corresponding weights ($w_{ij}$), and subsequently incorporating the bias ($b_j$), as represented by the following equation:

$$u = \sum_{i} w_{ij} x_i + b_j \tag{12}$$

In this context, $x_i$ corresponds to the output originating from the $i$ th neuron or node in the preceding layer, while $w_{ij}$ denotes the weight associated with the connection between the $i$ th and $j$-th layers, and $b_j$ signifies the bias present within the $j$-th layer. These activation functions introduce non-linear characteristics to the DNN, enabling it to encompass intricate relationships between the input features and the anticipated output. In the context of this study, weights and biases are regarded as parameters or variables subject to optimization, a process facilitated by previously discussed of EMA. As depicted in Fig. 7, the total number of variables to be optimized is calculated as follows: 3 inputs x 5 wt + 5 biases + 5 neurons x 5 wt + 5 biases + 5 neurons x 1 output + 1 bias = 56 variables.

In this paper, the fitness evaluation or objective function to be minimized is Mean Squared Error (MSE) metric, which is minimized during the optimization, which is expressed as follows:

$$MSE = \frac{1}{N} \sum_{i=1}^{N} (y_i - \widehat{y}_i)^2 \tag{13}$$

where

$\widehat{y}_i$- predicted

$y_i$- actual

$N$-number of observations.

Subsequently, the EMA-DNN model then is tested using a separate set of test data which has been presented previously. This training and validation processes for optimizing the weights and biases are repeated for ten times, and the results are recorded. The focus is on capturing the best optimal results, as well as evaluating the performance using metrics such as MSE, Mean Absolute Error (MAE), maximum error (MAX) and standard deviation (STD DEV). The metric of MAE is expressed as follows:

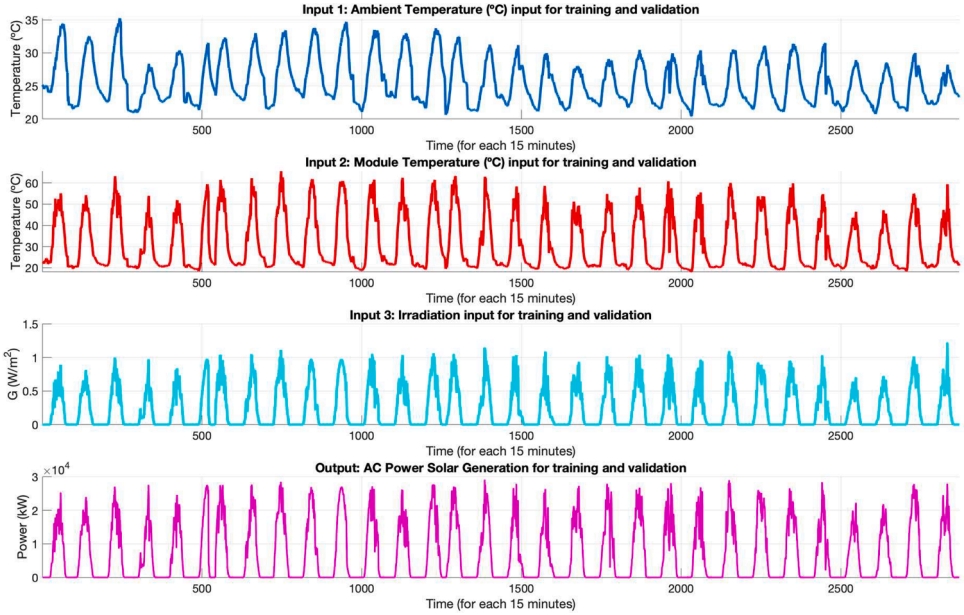


**Fig. 5.** Input-Output (31 days data) for training and validation processes.

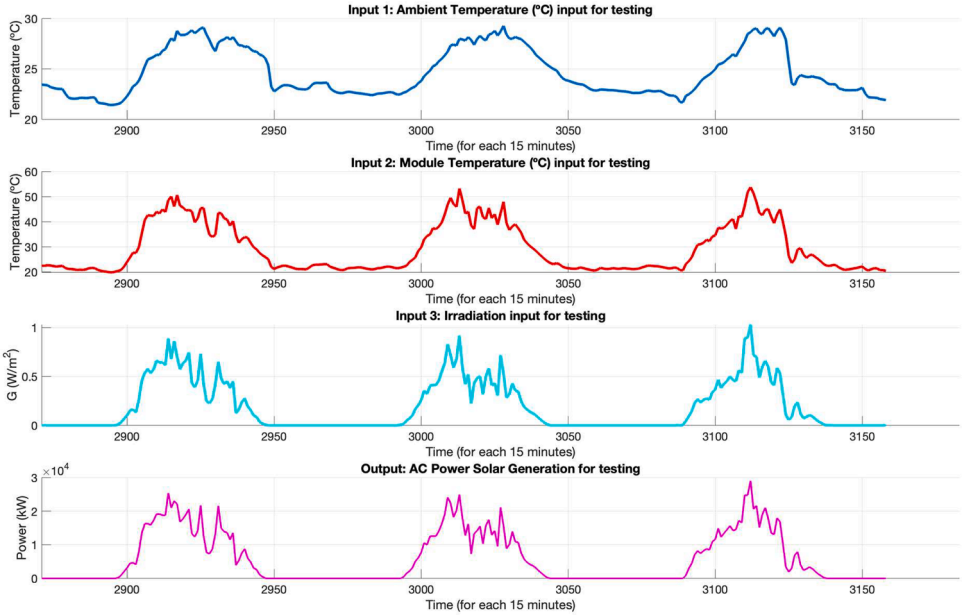


**Fig. 6.** Input-Output (3-day data) for testing process.

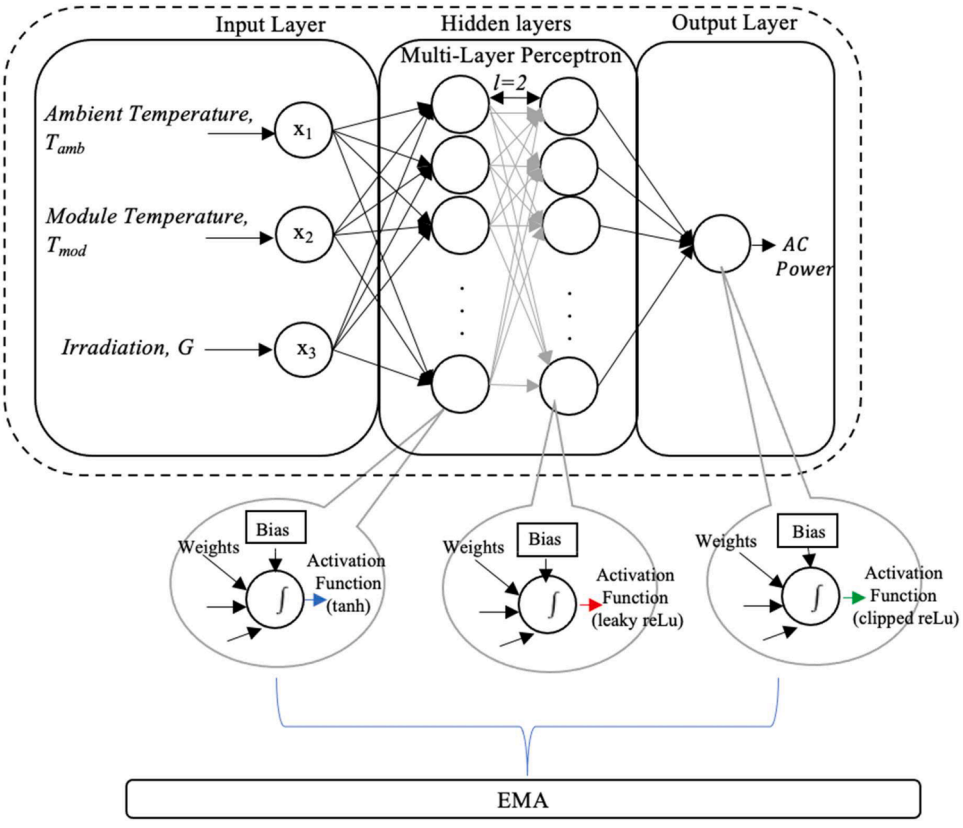


**Fig. 7.** Deep learning neural networks (DNN) architecture.

$$MAE = \frac{1}{N}\sum_{i=1}^{N}|y_i - \hat{y}_i| \tag{14}$$

In this study, the determination of the optimal number of neurons within each hidden layer, as well as the suitable number of hidden layers, was executed through a series of empirical experiments. It is crucial to emphasize that employing too few neurons could lead to inadequate learning, resulting in underfitting, while an excessive number of neurons could cause overfitting and hinder generalization. This underscores the significance of empirically determining the number of neurons within each hidden layer. Following a sequence of simulations and experimental iterations, a configuration comprising two hidden layers was chosen. The number of neurons in each hidden layer was systematically varied, specifically set to 3, 5, and 7. The performance metrics derived from five simulation runs for the identified hidden neuron counts are depicted in Fig. 8, where the optimal outcome

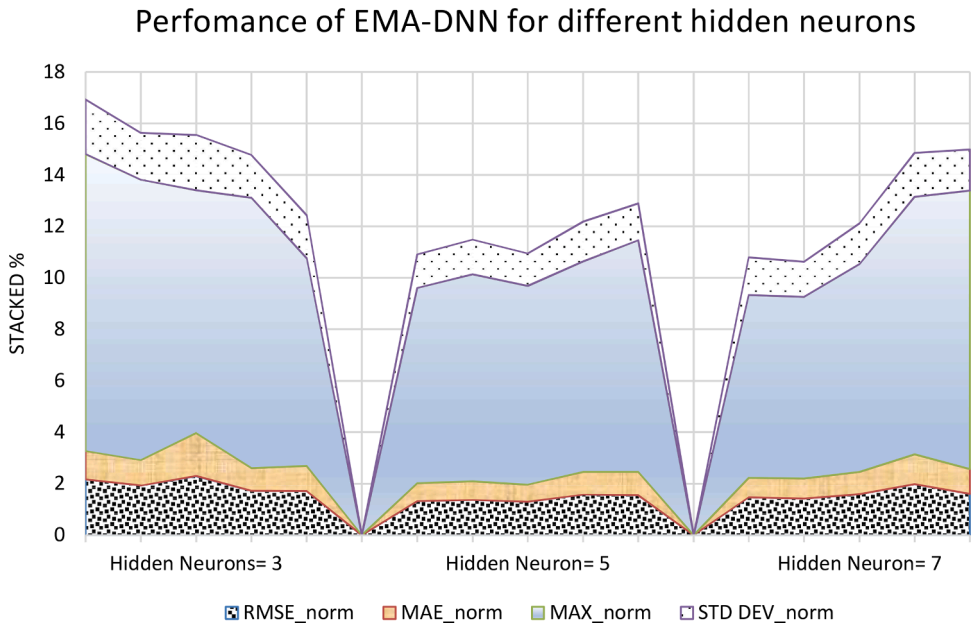


**Fig. 8.** Performance metrics for two hidden layers for various number of neurons using EMA-DNN for 5 simulation runs.

distinctly emerged for 5 neurons. Consequently, it can be deduced that a DNN architecture consisting of two hidden layers with 5 neurons each, yielded the most favorable outcomes across all evaluation metrics.

The flowchart in Fig. 9 outlines the process of optimizing the weights and biases of the EMA-DNN for predicting PV AC power output. The flowchart begins by loading the PV data, which is used for training, validation, and testing purposes. The next step involves the initialization phase, where the weights and biases of the DNN are generated randomly. Subsequently, new offspring are generated based on the selected candidates. These operations are part of the iterative process that continues until the maximum iteration limit is reached. During the optimization process, checks are in place to identify solutions that go beyond predefined bounds. If a solution exceeds these defined boundaries, it is constrained to remain within the boundaries to ensure feasibility and adherence to constraints. Once the maximum iteration is reached, the optimized weights and biases are recorded. Following this, the optimized weights and biases obtained by the EMA-DNN model are tested using a separate set of test data. This testing process is repeated ten times, and the results are documented.

## 6. RESULTS and discussion

The simulations in this paper were carried out utilizing MATLAB 2019b on a MacBook Pro-featuring a 2.40 GHz Quad-Core Intel Core i5 processor and 8 GB RAM. Table 1 presents the parameter settings used in this study for the EMA together with the other selected metaheuristic algorithms, viz. Differential Evolution (DE), Barnacles Mating optimizer (BMO), Particle Swarm Optimization (PSO) and Harmony Search Algorithm (HSA), allowing for fair performance comparisons. The maximum number of iterations was set to 250, and the population size was set to 30. It can be noted that the parameters for ADAM optimizer also has been presented in this table, where the maximum epochs is set to 1000 for obtaining comparable performance with the mentioned approaches. In order to evaluate the effectiveness of the EMA and other

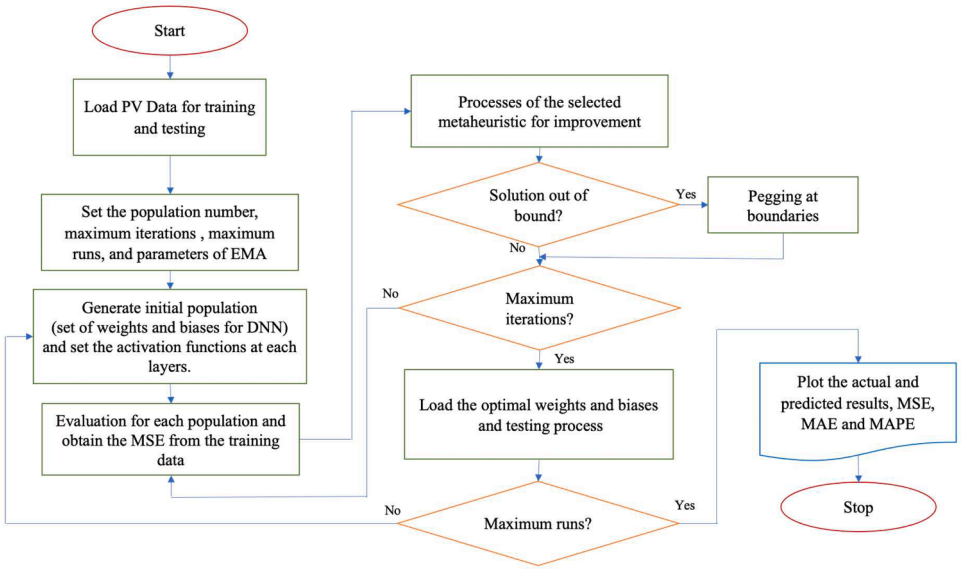


**Fig. 9.** Flow of EMA-DNN for forecasting the PV AC power output.

**Table 1**
Parameter setting used for all algorithms.

| Algorithm | Parameter setting |
|---|---|
| **# all algorithms** | Population size =30, maximum iteration =250, Simulation runs =10 |
| EMA | $Cr$= 0.5, $r < 0.45$ |
| DE | Crossover probability =0.8, Lower Bound of Scaling Factor: $\beta_{min}$= 0.2 Upper Bound of Scaling Factor: $\beta_{max}$= 0.8 |
| BMO | $pl$= 21 |
| PSO | $w$ = 0.7, $w_{damp}$=1, $c_1$= 1.5 $c_2$= 2 |
| HSA | Harmony Memory Consideration Rate: $HMCR$=0.9<br>Pitch Adjustment Rate: $PAR$=0.1<br>Fret Width (Bandwidth): $FW$=0.02*(Max value of variable-Min value of variable)<br>Fret Width Damp Ratio: $FW\_damp$=0.995% |
| ADAM | Maximum epochs = 1000,<br>$beta_1$ = 0.9;<br>$beta_2$ = 0.999;<br>$epsilon$ = $1 \times 10^{-8}$;<br>$learning\ rate$ = 0.01; |

algorithms in finding the optimal values of weights and biases for the DNN, multiple simulations were performed. Each algorithm was executed 10 times to assess its robustness, considering that the initialization process involves random number generation. This approach allows us to analyze the performance and reliability of the DNN model across different runs and validate the effectiveness of the metaheuristic algorithms.

Table 2 provides a comprehensive overview of the performance of various metaheuristic-DNN algorithms, as evaluated through mean squared error (MSE), mean absolute error (MAE), maximum error (MAX), and standard deviation (STD DEV) metrics over 10 simulation runs. Notably, this table presents dual perspectives, incorporating both normalized and actual data outcomes. The significance of these results lies in their revelation of the profound impact of the Evolutionary Mating Algorithm (EMA) and other comparative algorithms. The utilization of normalized data during the training and validation phases underscores the utility of regularization and stable learning in the process. Meanwhile, the inclusion of actual forecasted data in the table highlights the intricate challenges posed by forecasting PV AC power generation. This complexity arises from the substantial fluctuations between zero kW and thousands of kilowatts, underscoring the inherent intricacies of PV generation prediction. The presentation of these divergent data sets serves to underscore not only the formidable task of accurate forecasting, but also its potential implications for enhanced grid management.

The table presents a comprehensive evaluation of the performance of various metaheuristic-DNN algorithms in predicting PV AC power output, considering key metrics such as RMSE, MAE, MAX, and STD DEV over 10 simulation runs. The findings highlight distinctive trends across the algorithms. The EMA-DNN emerges as a promising approach, achieving the best results in terms of RMSE, MAE, and MAX. It demonstrates the ability to yield relatively accurate predictions, with a lowest RMSE of 374.40, MAE of 201, and MAX of 2128.80. Moreover, the standard deviation of its predictions is comparably lower, suggesting consistent performance across simulations. In contrast, the DE-DNN, while still providing relatively competitive results, exhibits higher values in RMSE, MAE, and MAX compared to EMA-DNN. This indicates that while DE-DNN can offer decent forecasts, it is less precise in terms of error minimization.

The BMO-DNN showcases performance falling between EMA-DNN and DE-DNN. It achieves RMSE, MAE, and MAX values that are closer to those of EMA-DNN. However, it also exhibits some variability in performance, as evidenced by its higher standard deviation values. The PSO-DNN stands out as another promising contender, securing relatively lower RMSE and MAE values compared to DE-DNN and BMO-DNN. This suggests that PSO-DNN can provide improved predictions and a better balance between accuracy and error minimization. Lastly, the HSA-DNN tends to yield relatively higher errors across all metrics compared to the other algorithms, indicating that its predictive capacity might be somewhat limited.

Considering the results of DNN with ADAM optimizer and NARX, it is noteworthy that EMA-DNN continues to outperform other algorithms in terms of accuracy. DNN with ADAM optimizer, on the other hand, exhibits significantly higher errors, both in normalized and actual metrics, reaffirming the limitations of gradient-based optimization methods in this context. The inclusion of NARX, designed for time series forecasting, shows that it falls short in accuracy compared to metaheuristic-DNN approaches, with higher errors across all metrics. These additional findings further underscore the superiority of EMA-DNN in tackling the challenges posed by PV AC power generation prediction, validating the efficacy of the evolutionary mating algorithm in enhancing deep neural network performance for this specific task.

The evaluation of the metaheuristic-DNN algorithms' performance in predicting PV AC power output becomes more nuanced when considering the results of normalized key metrics. These metrics provide insight into the algorithms' ability to generalize their predictions across different ranges of data. Across the board, when normalized data is utilized, the algorithms generally exhibit improved performance in terms of RMSE, MAE, and MAX. Notably, the EMA-DNN maintains its superiority, achieving the lowest normalized RMSE of 1.28, indicating its capability to consistently generate predictions close to the actual

**Table 2**
Performances of metaheuristic-DNN for PV output current prediction.

| Algorithm/ Performance metric | | RMSE | MAE | MAX | STD DEV | RMSE_norm | MAE_norm | MAX_norm | STD DEV_norm |
|---|---|---|---|---|---|---|---|---|---|
| EMA-DNN | Best | 374.40 | 201.00 | 2128.80 | 374.10 | 1.28 | 0.69 | 7.30 | 1.28 |
| | Worst | 458.7 | 255.1 | 2387.7 | 450.6 | 1.57 | 0.88 | 8.19 | 1.55 |
| | Mean | 406.88 | 215.59 | 2353.06 | 397.39 | 1.40 | 0.74 | 8.07 | 1.36 |
| DE-DNN | Best | 558.03 | 355.11 | 2251.73 | 533.59 | 1.91 | 1.22 | 7.72 | 1.83 |
| | Worst | 845.51 | 473.31 | 3950.63 | 836.47 | 2.90 | 1.62 | 13.55 | 2.87 |
| | Mean | 664.48 | 405.36 | 2976.64 | 632.90 | 2.28 | 1.39 | 10.21 | 2.17 |
| BMO-DNN | Best | 463.2 | 254 | 2341.3 | 462.4 | 1.59 | 0.87 | 8.03 | 1.59 |
| | Worst | 669.3 | 336.6 | 3889 | 636.8 | 2.30 | 1.15 | 13.34 | 2.18 |
| | Mean | 577.39 | 326.11 | 2944.53 | 558.06 | 1.98 | 1.12 | 10.10 | 1.91 |
| PSO-DNN | Best | 395.2 | 196.3 | 2476.3 | 379.9 | 1.36 | 0.67 | 8.50 | 1.30 |
| | Worst | 613.2 | 366 | 3384.5 | 590.3 | 2.10 | 1.26 | 11.61 | 2.03 |
| | Mean | 449.94 | 236.99 | 2691.73 | 425.03 | 1.54 | 0.81 | 9.23 | 1.46 |
| HSA-DNN | Best | 612.98 | 459.18 | 2323.57 | 613.82 | 2.10 | 1.58 | 7.97 | 2.11 |
| | Worst | 967.59 | 552.19 | 4172.92 | 941.64 | 3.32 | 1.89 | 14.32 | 3.23 |
| | Mean | 783.57 | 485.05 | 3161.75 | 760.56 | 2.69 | 1.66 | 10.85 | 2.61 |
| DNN (ADAM) | Best | 1962.2 | 1544 | 5900.5 | 1449.6 | 6.73 | 5.30 | 20.24 | 4.97 |
| | Worst | 10,210 | 9952 | 16,358 | 2286 | 35.0262 | 34.14 | 56.12 | 7.84 |
| | Mean | 5593.11 | 4281.78 | 13,527.5 | 4034.83 | 19.19 | 14.69 | 46.41 | 13.84 |
| NARX | Best | 2321.57 | 1357.32 | 9813.77 | 2313.50 | 7.96 | 4.66 | 33.67 | 7.94 |

data. Similarly, EMA-DNN attains the lowest normalized MAE of 0.69, indicating its accuracy in predicting the magnitude of errors.

Comparatively, the other algorithms also show a trend of reduced normalized RMSE and MAE when normalized data is utilized. However, the gaps between their performance and that of EMA-DNN persist. The DE-DNN, BMO-DNN, PSO-DNN, HSA-DNN, DNN with ADAM and NARX still exhibit higher normalized error values than EMA-DNN, suggesting that while they improve with normalization, they are yet to match the superior accuracy of EMA-DNN.

Furthermore, normalized MAX values indicate that EMA-DNN also excels in predicting the most extreme deviations, as it maintains the lowest normalized MAX value of 7.30. This reflects its consistent performance in handling outliers or sharp peaks, often associated with PV AC power generation data. In conclusion, the utilization of normalized key metrics underscores the impressive performance of EMA-DNN in maintaining accuracy and minimizing errors across the entire range of PV AC power output data. While other algorithms also benefit from normalization, EMA-DNN stands out as a robust choice for predictive modelling in this context, as it demonstrates a consistently high level of accuracy even when faced with extreme data points.

In optimizing process, the convergence curves of the training process for all algorithms for minimizing the mean square error (MSE) is depicted in Fig. 10. It is observed that PSO-DNN exhibits the best convergence, reaching the minimum MSE value within 250 iterations. On the other hand, HSA-DNN shows the worst convergence and struggles to reach a low MSE value even approaching 250 iterations. In terms of convergence performance, EMA-DNN and BMO-DNN demonstrate similar behavior, converging at a moderate pace and achieving reasonably low MSE values. However, when comparing the prediction performance based on the testing results in Table 2, it is evident that EMA-DNN outperforms others. EMA-DNN achieves the lowest MSE, MAE, and MAX values among all the metaheuristic-DNN algorithms, indicating its superior predictive accuracy for PV AC power output prediction.

Interestingly, despite PSO-DNN exhibiting the best convergence during the training process, it does not translate into the best prediction performance in the testing phase. PSO-DNN yields relatively higher MSE, MAE, and MAPE values compared to EMA-DNN and ranked in second best if RMSE is used for benchmarked. This suggests that PSO-DNN may require further iterations or adjustments to enhance its generalization capability and improve its predictive accuracy on unseen test data. Thus, EMA-DNN is recommended as the preferred metaheuristic optimization algorithm for optimizing the weights and biases of the DNN model in the context of PV AC power output prediction.

Figs. 11 to 17 portray the detailed outcomes of the projected and actual PV AC power output generated by the EMA-DNN, DE-DNN, BMO-DNN, PSO-DNN, HSA-DNN, DNN (ADAM) and NARX approaches. These figures additionally feature the error, accompanied by the corresponding instance timestamp. These findings offer valuable insights into the precision of the forecasted results when compared to the actual data. Among the various metaheuristic-DNN strategies, it is evident that EMA-DNN showcases the most impressive performance in mirroring the test data's patterns. The predicted values align closely with the actual values, indicating a substantial capability to capture the underlying trends and dynamics. The maximal error attributed to EMA-DNN stands at 7.303 % (in terms of normalized value), pinpointing this occurrence at sample time #61 as illustrated in Fig. 11. This signifies that although EMA-DNN might exhibit minor deviations from the actual value in this specific instance, its overall accuracy remains considerably high.

In contrast, HSA-DNN exhibits the weakest performance among the algorithms, with a maximum error of 7.9 % observed at sample time #61. Generally, a significant discrepancy becomes evident between the predicted and actual values, suggesting that HSA-DNN encounters challenges in precisely capturing the intricate relationships within the PV AC power output data. On the whole, the comprehensive examination of results from Figs. 11,12,13,14,15,16,17 underscores the remarkable performance of EMA-DNN in terms of accurately following the patterns within the test data. This observation reinforces the conclusions drawn from the performance evaluation highlighted in Table 2, where EMA-DNN achieves the lowest MSE, MAE, and MAX values.

Table 3 illustrates the performance of the metaheuristic-DNN algorithms in predicting PV AC power output for two specific sample ranges:

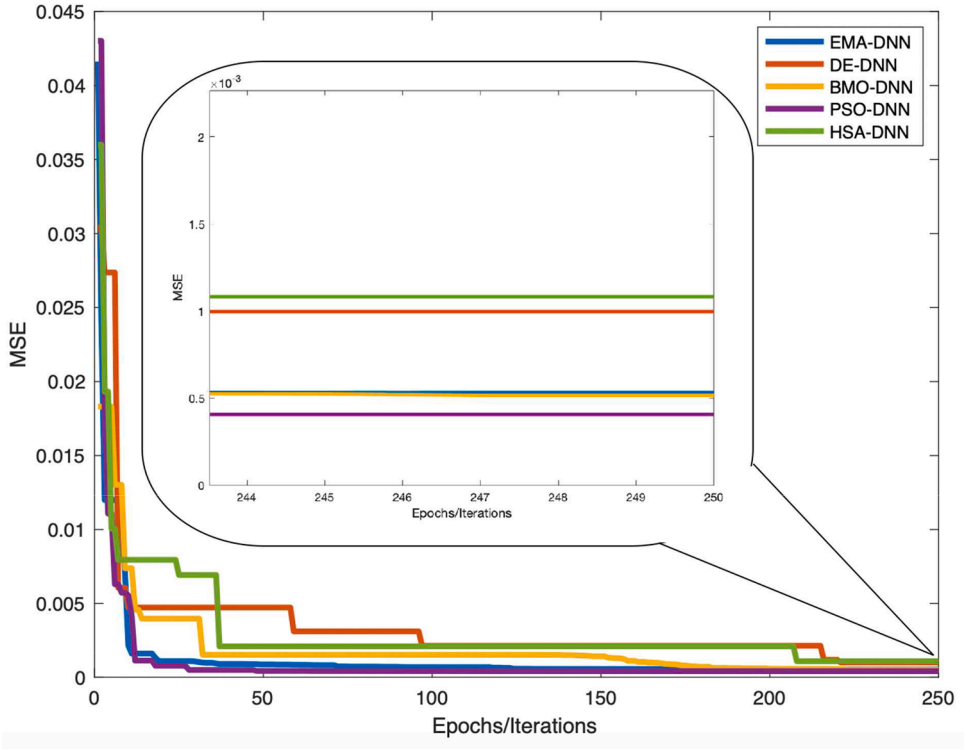


**Fig. 10.** Convergence curves of all optimizers for training process.

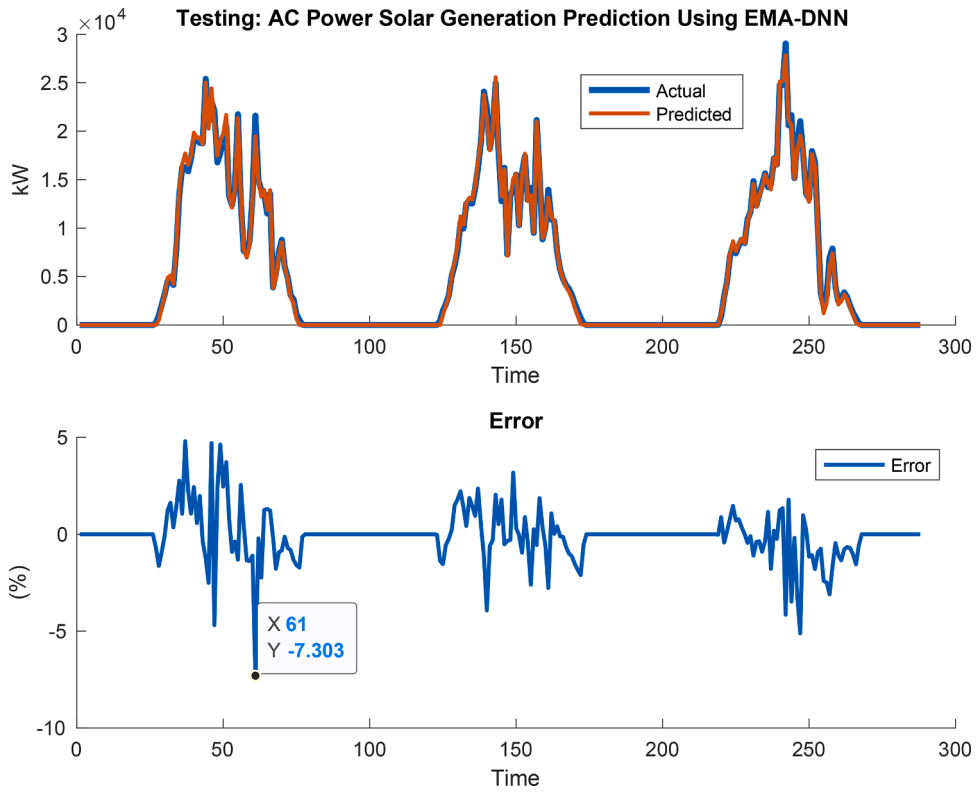


**Fig. 11.** The best of PV AC power output prediction obtained by EMA-DNN.

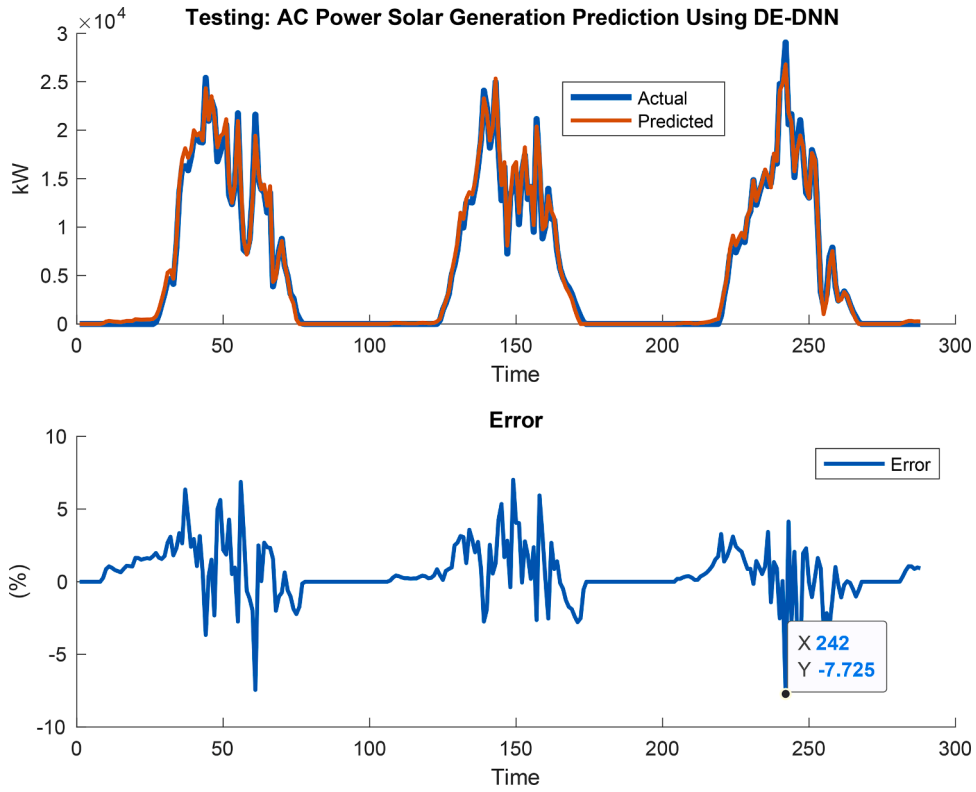


**Fig. 12.** The best of PV AC power output prediction obtained by DE-DNN.

#60 to #74 and #240 to #250. The table encompasses both the actual AC power generation values and the corresponding predictions provided by each algorithm. The primary aim of this table is to visually portray the maximum errors or disparities detected by all algorithms, as highlighted in bold. By referencing Fig. 11,12, 13, 14, 15, 16, 17, these discrepancies become evident. Notably, the presented results are in their

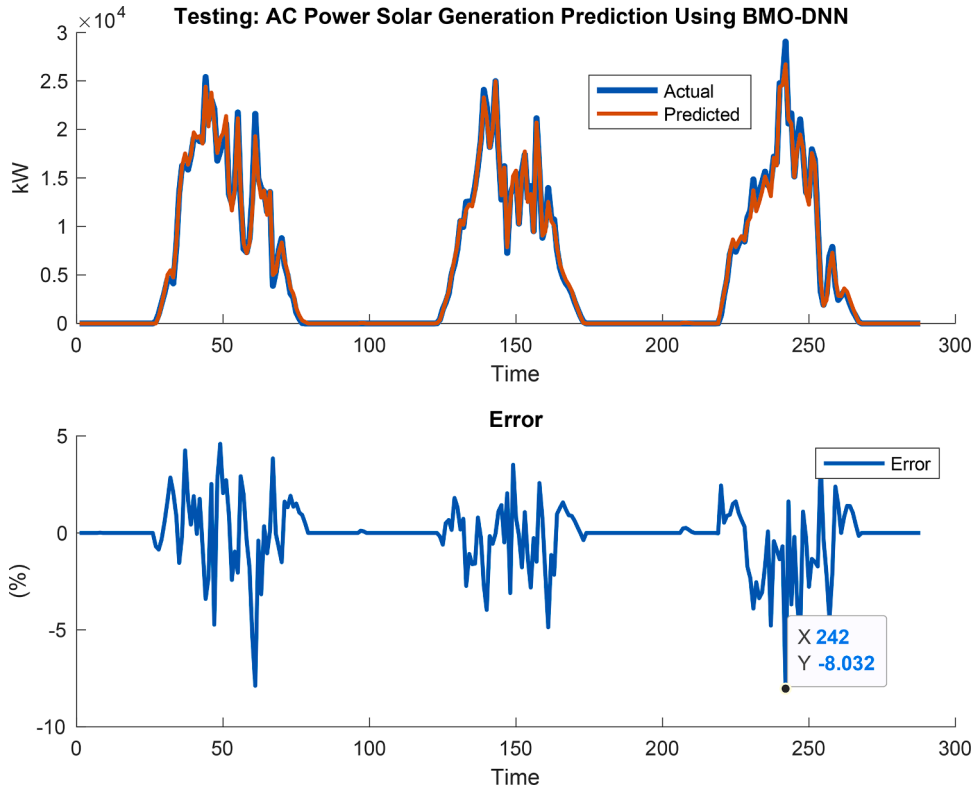


**Fig. 13.** The best of PV AC power output prediction obtained by BMO-DNN.

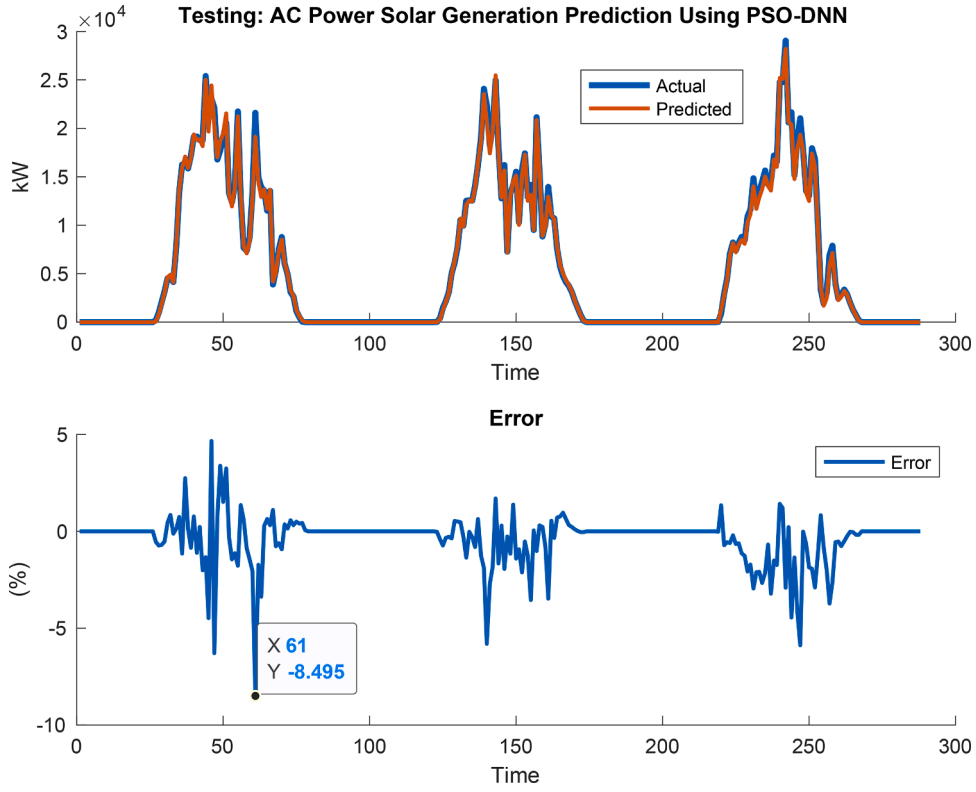


**Fig. 14.** The best of PV AC power output prediction obtained by PSO-DNN.

original, non-normalized form. This depiction underscores the substantial variation errors associated with the predicted values across all algorithms. This observation emphasizes the need for potential enhancements in future prediction endeavors, particularly in the context of refining grid management. These improvements could have various applications, such as aiding in maintenance activities, identifying faulty

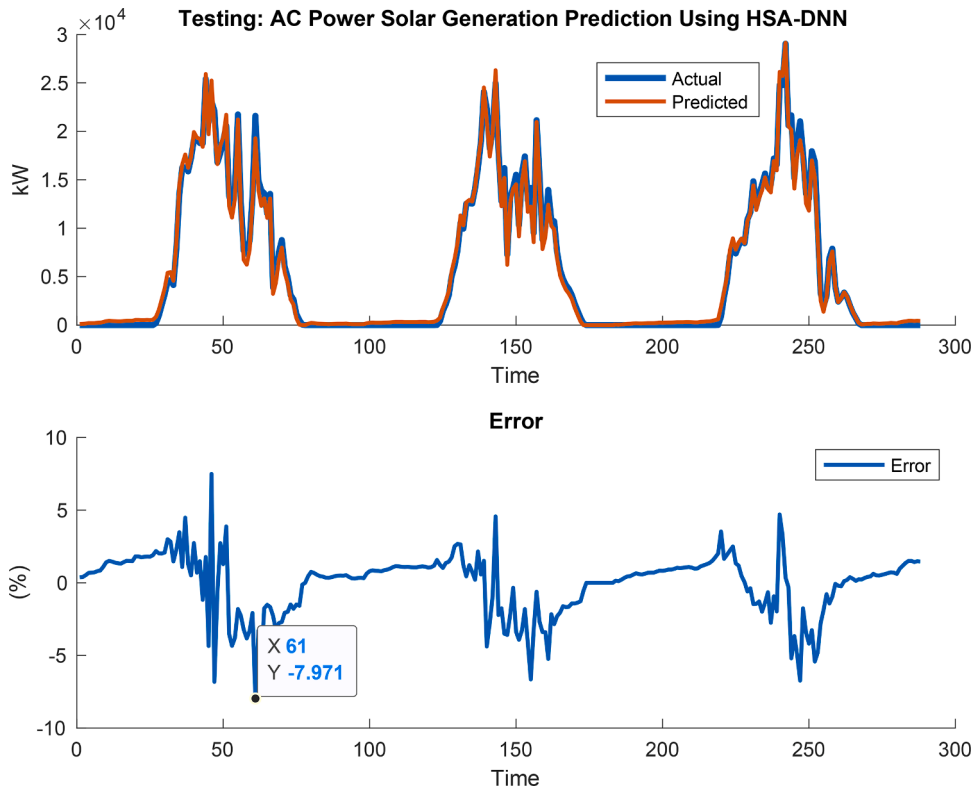


**Fig. 15.** The best of PV AC power output prediction obtained by HSA-DNN.

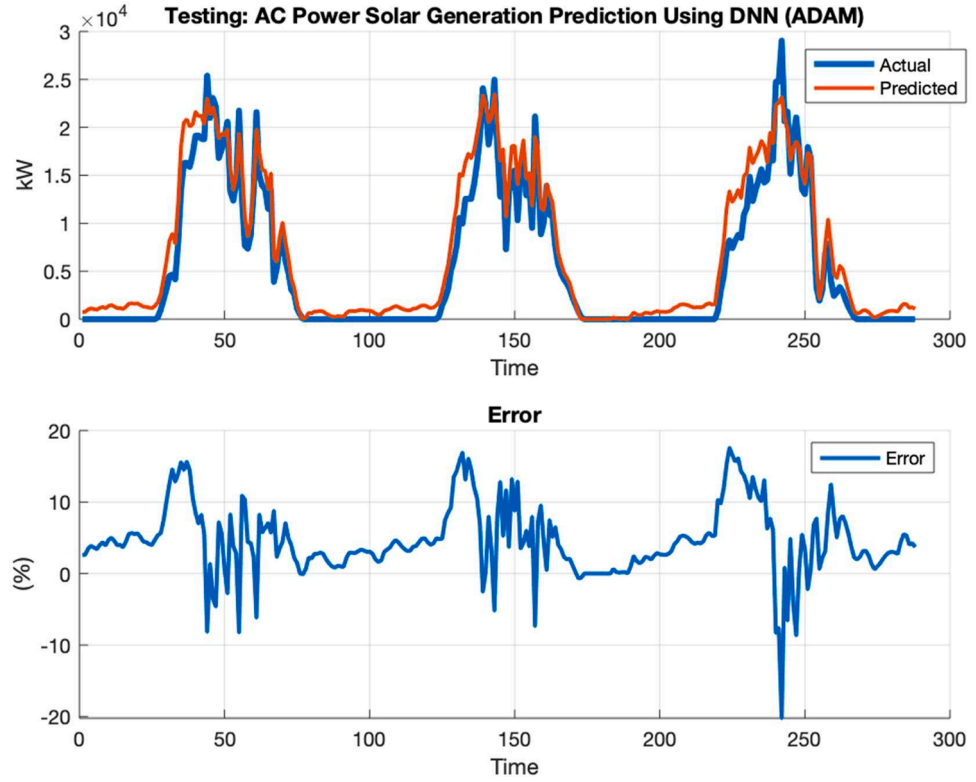


**Fig. 16.** The best of PV AC power output prediction obtained by DNN (ADAM).

or suboptimal equipment, and supporting overall operational efficiency.

Finally, Fig. 18 offers a comprehensive comparison of PV AC power generation curves for all the metaheuristic-DNN models, for the first testing day underscoring their respective performances. The examination distinctly illustrates that EMA-DNN outperforms the other selected metaheuristic-DNN models in accurately forecasting the PV output

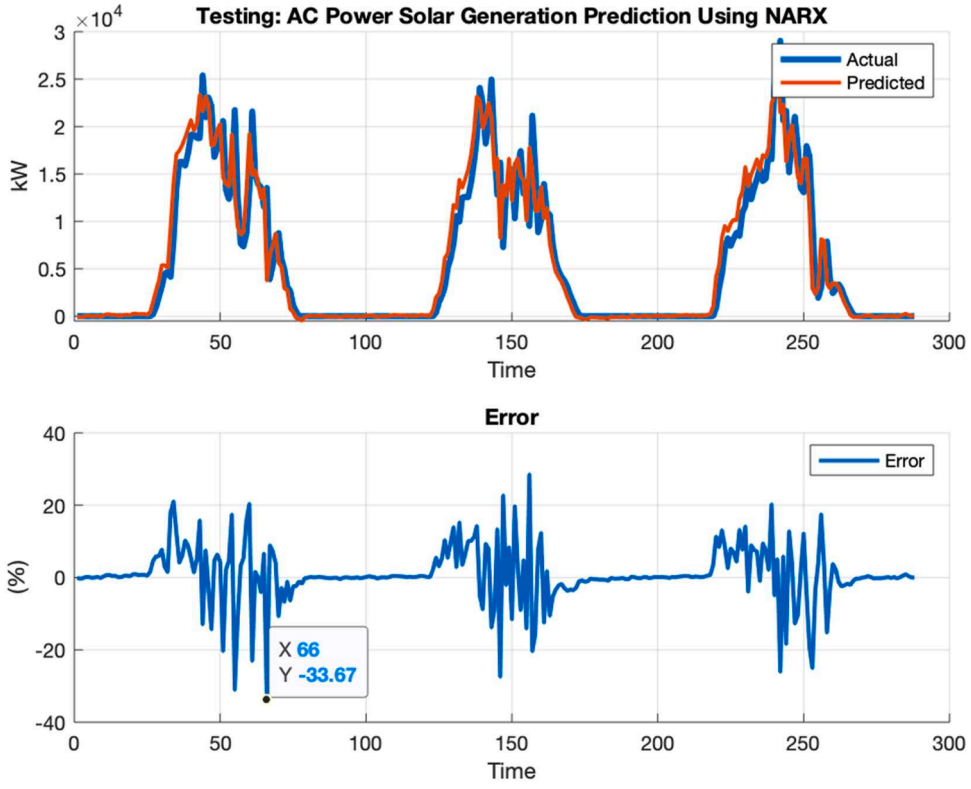


**Fig. 17.** The best of PV AC power output prediction obtained by Nonlinear AutoRegressive with eXogenous inputs (NARX).

**Table 3**
Samples of metaheuristic-DNN for PV AC power output prediction.

| Sample # | Actual | EMA-DNN | DE-DNN | BMO-DNN | PSO-DNN | HSA-DNN | DNN(ADAM) | NARX |
|---|---|---|---|---|---|---|---|---|
| 60 | 13,288 | 12,966 | 12,716 | 11,709 | 12,693 | 12,681 | 13,985 | 19,232 |
| 61 | 21,599 | **19,471** | 19,428 | 19,303 | **19,123** | **19,276** | 19,793 | 14,861 |
| 62 | 14,927 | 14,864 | 15,653 | 14,810 | 14,423 | 13,963 | 17,333 | 15,403 |
| 63 | 13,901 | 13,248 | 13,913 | 12,980 | 12,918 | 12,311 | 15,578 | 13,891 |
| 64 | 13,595 | 13,960 | 14,375 | 13,694 | 13,676 | 13,081 | 15,457 | 12,396 |
| 65 | 11,505 | 11,885 | 12,196 | 11,199 | 11,688 | 11,063 | 13,562 | 13,432 |
| 66 | 13,544 | 13,900 | 14,221 | 13,578 | 13,636 | 13,060 | 15,208 | 3731 |
| 67 | 3885 | 3844 | 4343 | 5005 | 4207 | 3226 | 6443 | 6489 |
| 68 | 5327 | 4807 | 4744 | 5317 | 5102 | 4379 | 5998 | 7454 |
| 69 | 7545 | 7275 | 7246 | 7319 | 7366 | 6736 | 8575 | 8735 |
| 70 | 8776 | 8533 | 8554 | 8337 | 8506 | 7989 | 10,079 | 5644 |
| 71 | 6028 | 5990 | 6212 | 6499 | 6133 | 5427 | 8088 | 5205 |
| 72 | 4900 | 4694 | 4724 | 5285 | 4943 | 4316 | 6350 | 2914 |
| 73 | 3086 | 2847 | 2786 | 3642 | 3252 | 2649 | 4241 | 2763 |
| 74 | 2641 | 2255 | 2095 | 3036 | 2733 | 2118 | 3284 | 767 |
| 75 | 1137 | 676 | 487 | 1577 | 1282 | 699 | 1571 | 430 |
| : | : | : | : | : | : | : | : | : |
| 240 | 24,774 | 25,133 | 24,038 | 24,377 | 25,188 | 26,142 | 22,353 | 23,319 |
| 241 | 24,771 | 25,163 | 24,784 | 24,570 | 25,122 | 25,729 | 22,548 | 26,265 |
| 242 | 29,049 | 27,839 | **26,797** | **26,707** | 28,200 | 29,150 | 23,148 | 21,438 |
| 243 | 20,619 | 21,140 | 21,825 | 21,091 | 20,682 | 20,531 | 20,863 | 22,335 |
| 244 | 21,656 | 20,643 | 20,828 | 20,580 | 20,359 | 20,141 | 19,732 | 16,283 |
| 245 | 15,160 | 15,106 | 15,759 | 15,099 | 14,765 | 14,088 | 16,583 | 18,908 |
| 246 | 19,014 | 18,064 | 17,992 | 17,942 | 17,802 | 17,554 | 17,756 | 20,184 |
| 247 | 21,044 | 19,554 | 19,455 | 19,476 | 19,330 | 19,082 | 18,519 | 17,320 |
| 248 | 17,746 | 18,030 | 18,314 | 18,065 | 17,741 | 17,232 | 17,870 | 14,694 |
| 249 | 13,531 | 13,597 | 14,199 | 13,451 | 13,340 | 12,530 | 15,122 | 13,954 |
| 250 | 13,048 | 12,711 | 13,031 | 12,239 | 12,507 | 11,827 | 14,076 | 16,610 |
| RMSE | | 374.40 | 558.03 | 463.20 | 395.20 | 612.98 | 1962.20 | 2321.57 |

current. This observation corroborates the preceding discussions and solidifies the superiority of EMA-DNN. Additionally, the PSO-DNN model exhibits promising outcomes and emerges as the second-best performer within the evaluated models. Conversely, the performance of other metaheuristic-DNN models, including DE-DNN, BMO-DNN, and HSA-DNN, as well as DNN with ADAM optimizer and NARX lags slightly behind. Despite not reaching the same accuracy level in predicting PV AC power generation, these models still present viable alternatives for addressing the prediction task.

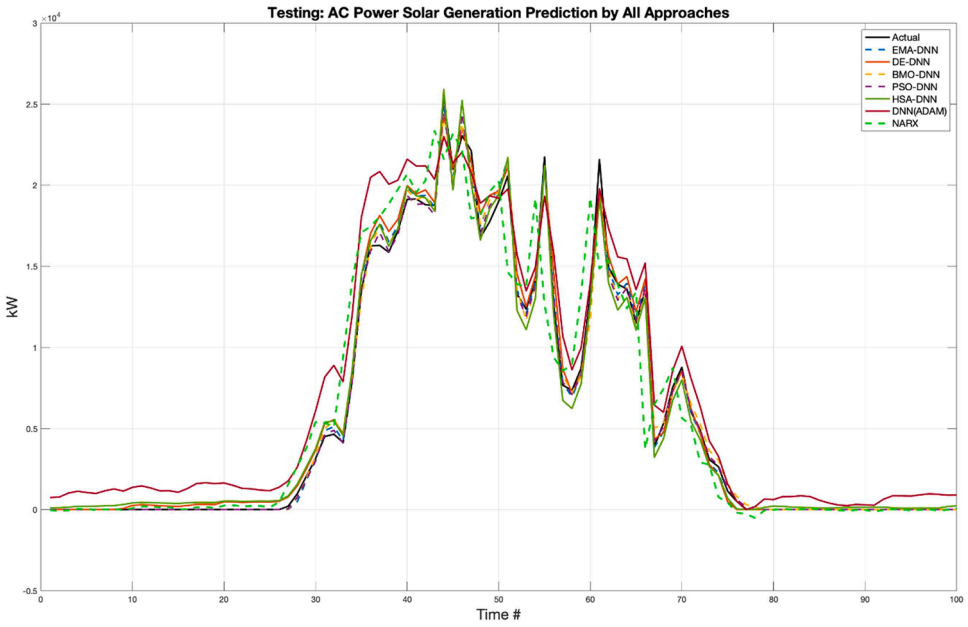


**Fig. 18.** Comparison performances of all approaches for PV output current prediction.

## 7. Conclusion

In conclusion, this study presented an innovative approach that integrates the Evolutionary Mating Algorithm (EMA) with Deep Neural Networks (DNN) to enhance the accuracy of PV AC power generation forecasting. The investigation delved into a dataset collected from solar power plants in India, spanning 34 days with 15-minute intervals. The data included parameters like solar irradiation, ambient temperature, module temperature, and AC power output. Pre-processing steps involved normalization to facilitate efficient DNN training. The core of the approach centered around the EMA-DNN optimization framework. The EMA played a crucial role in optimizing DNN weights and biases. The experimentation encompassed diverse facets, including hidden layer architecture determination and metaheuristic optimizer evaluation. Empirical evaluation highlighted the superior accuracy of the EMA-DNN model compared to other state-of-the-art metaheuristic-DNN approaches. The comprehensive comparison revealed the proficiency of the proposed approach in tracking and predicting PV AC power generation. The EMA-DNN model consistently outperformed others based on metrics like mean squared error, mean absolute error, maximum error, and standard deviation. This validation underscores the potential and effectiveness of our proposed approach.

In essence, this research provides insights into the synergistic blend of evolutionary algorithms and deep learning for precise solar power generation forecasting. The findings emphasize the viability of the EMA-DNN approach in enhancing grid management and optimizing renewable energy utilization. As the energy landscape evolves, this study contributes to harnessing renewable energy potential using cutting-edge optimization techniques. Future research avenues could explore refining the approach, exploring larger datasets, and addressing real-time prediction challenges.

## CRediT authorship contribution statement

**Mohd Herwan Sulaiman:** Writing – original draft, Visualization, Software, Methodology, Investigation, Formal analysis, Data curation, Conceptualization. **Zuriani Mustaffa:** Writing – review & editing, Validation, Investigation, Formal analysis.

## Declaration of competing interest

The authors declare that they have no known competing financial interests or personal relationships that could have appeared to influence the work reported in this paper.

## Data availability

Data can be obtained from https://www.kaggle.com/datasets/ani-kannal/solar-power-generation-data

## Acknowledgments

This work was supported by the Ministry of Higher Education Malaysia (MOHE) under Fundamental Research Grant Scheme (FRGS/1/2022/ICT04/UMP/02/1) and Universiti Malaysia Pahang Al-Sultan Abdullah (UMPSA) under Distinguished Research Grant (#RDU223003).

## References

[1] Antonanzas J, Osorio N, Escobar R, Urraca R, Martinez-de-Pison FJ, Antonanzas-Torres F. Review of photovoltaic power forecasting. Solar Energy 2016;136:78–111. https://doi.org/10.1016/j.solener.2016.06.069. 2016/10/15/.

[2] Zheng J, Zeng B. Unleashing the influencing factors of solar energy adoption to combat climate change: a roadmap toward sustainable energy technologies. Sustainable Energy Technologies and Assessments 2023;57:103303. https://doi.org/10.1016/j.seta.2023.103303. 2023/06/01/.

[3] Pombo DV, Rincón MJ, Bacher P, Bindner HW, Spataru SV, Sørensen PE. Assessing stacked physics-informed machine learning models for co-located wind–solar power forecasting. Sustainable Energy, Grids and Networks 2022;32:100943. https://doi.org/10.1016/j.segan.2022.100943. 2022/12/01/.

[4] Cattani G. Combining data envelopment analysis and Random Forest for selecting optimal locations of solar PV plants. Energy and AI 2023;11:100222. https://doi.org/10.1016/j.egyai.2022.100222. 2023/01/01/.

[5] Khan UA, Khan NM, Zafar MH. Resource efficient PV power forecasting: transductive transfer learning based hybrid deep learning model for smart grid in Industry 5.0. Energy Conversion and Management: X 2023;20:100486. https://doi.org/10.1016/j.ecmx.2023.100486. 2023/10/01/.

[6] Verma P, Kaur T. Power reserve control strategy of PV system for active power reserve under dynamic shading patterns. Array 2022;16:100250. https://doi.org/10.1016/j.array.2022.100250. 2022/12/01/.

[7] S. Cantillo-Luna, R. Moreno-Chuquen, D. Celeita, and G. Anders, "Deep and Machine Learning Models to Forecast Photovoltaic Power Generation," *Energies*, vol. 16, no. 10, https://doi.org/10.3390/en16104097.

[8] L. Liu and Y. Li, "Research on a Photovoltaic Power Prediction Model Based on an IAO-LSTM Optimization Algorithm," *Processes*, vol. 11, no. 7, https://doi.org/10.3390/pr11071957.

[9] L. Liu et al., "A Photovoltaic Power Prediction Approach Based on Data Decomposition and Stacked Deep Learning Model," *Electronics (Basel)*, vol. 12, no. 13, https://doi.org/10.3390/electronics12132764.

[10] Abou Houran M, Salman Bukhari SM, Zafar MH, Mansoor M, Chen W. COA-CNN-LSTM: coati optimization algorithm-based hybrid deep learning model for PV/wind power forecasting in smart grid applications. Appl Energy 2023;349:121638. https://doi.org/10.1016/j.apenergy.2023.121638. 2023/11/01/.

[11] Ahmed R, Sreeram V, Mishra Y, Arif MD. A review and evaluation of the state-of-the-art in PV solar power forecasting: techniques and optimization. Renewable and Sustainable Energy Reviews 2020;124:109792. https://doi.org/10.1016/j.rser.2020.109792. 2020/05/01/.

[12] Kaur D, Islam SN, Mahmud MA, Haque ME, Anwar A. A VAE-Bayesian deep learning scheme for solar power generation forecasting based on dimensionality reduction. Energy and AI 2023;14:100279. https://doi.org/10.1016/j.egyai.2023.100279. 2023/10/01/.

[13] Ma X, et al. Predicting the utilization factor of blasthole in rock roadways by random forest. Underground Space 2023;11:232–45. https://doi.org/10.1016/j.undsp.2023.01.006. 2023/08/01/.

[14] Kim HJ, Kim MK. A novel deep learning-based forecasting model optimized by heuristic algorithm for energy management of microgrid. Appl Energy 2023;332:120525. https://doi.org/10.1016/j.apenergy.2022.120525. 2023/02/15/.

[15] Memarzadeh G, Keynia F. A new hybrid CBSA-GA optimization method and MRMI-LSTM forecasting algorithm for PV-ESS planning in distribution networks. Journal of Energy Storage 2023;72:108582. https://doi.org/10.1016/j.est.2023.108582. 2023/11/30/.

[16] Sayed ET, et al. Application of artificial intelligence techniques for modeling, optimizing, and controlling desalination systems powered by renewable energy resources. J Clean Prod 2023;413:137486. https://doi.org/10.1016/j.jclepro.2023.137486. 2023/08/10/.

[17] Song Z, Cao S, Yang H. Assessment of solar radiation resource and photovoltaic power potential across China based on optimized interpretable machine learning model and GIS-based approaches. Appl Energy 2023;339:121005. https://doi.org/10.1016/j.apenergy.2023.121005. 2023/06/01/.

[18] Boriratrit S, Fuangfoo P, Srithapon C, Chatthaworn R. Adaptive meta-learning extreme learning machine with golden eagle optimization and logistic map for forecasting the incomplete data of solar irradiance. Energy and AI 2023;13:100243. https://doi.org/10.1016/j.egyai.2023.100243. 2023/07/01/.

[19] Ashraf WM, Dua V. Machine learning based modelling and optimization of post-combustion carbon capture process using MEA supporting carbon neutrality. Digital Chemical Engineering 2023;8:100115. https://doi.org/10.1016/j.dche.2023.100115. 2023/09/01/.

[20] Chou J-S, Nguyen N-M, Chang C-P. Intelligent candlestick forecast system for financial time-series analysis using metaheuristics-optimized multi-output machine learning. Appl Soft Comput 2022;130:109642. https://doi.org/10.1016/j.asoc.2022.109642. 2022/11/01/.

[21] Alasmari N, et al. Improved metaheuristics with deep learning based object detector for intelligent control in autonomous vehicles. Computers and Electrical Engineering 2023;108:108718. https://doi.org/10.1016/j.compeleceng.2023.108718. 2023/05/01/.

[22] Abdullah Alohali M, et al. Metaheuristics with deep learning driven phishing detection for sustainable and secure environment. Sustainable Energy Technologies and Assessments 2023;56:103114. https://doi.org/10.1016/j.seta.2023.103114. 2023/03/01/.

[23] Davoodi S, Vo Thanh H, Wood DA, Mehrad M, Rukavishnikov VS. Combined machine-learning and optimization models for predicting carbon dioxide trapping indexes in deep geological formations. Appl Soft Comput 2023;143:110408. https://doi.org/10.1016/j.asoc.2023.110408. 2023/08/01/.

[24] Huang Q, Ding H, Sheykhahmad FRashid. A skin cancer diagnosis system for dermoscopy images according to deep training and metaheuristics. Biomed Signal Process Control 2023;83:104705. https://doi.org/10.1016/j.bspc.2023.104705. 2023/05/01/.

[25] Suddle MK, Bashir M. Metaheuristics based long short term memory optimization for sentiment analysis. Appl Soft Comput 2022;131:109794. https://doi.org/10.1016/j.asoc.2022.109794. 2022/12/01/.

[26] Drewil GI, Al-Bahadili RJ. Air pollution prediction using LSTM deep learning and metaheuristics algorithms. Measurement: Sensors 2022;24:100546. https://doi.org/10.1016/j.measen.2022.100546. 2022/12/01/.

[27] khelili MA, slatnia S, kazar O, merizig A, mirjalili S. Deep learning and metaheuristics application in internet of things: a literature review. Microprocess Microsyst 2023;98:104792. https://doi.org/10.1016/j.micpro.2023.104792. 2023/04/01/.

[28] Qiao X, et al. Metaheuristic evolutionary deep learning model based on temporal convolutional network, improved aquila optimizer and random forest for rainfall-runoff simulation and multi-step runoff prediction. Expert Syst Appl 2023;229:120616. https://doi.org/10.1016/j.eswa.2023.120616. 2023/11/01/.

[29] Tameswar K, Suddul G, Dookhitram K. A hybrid deep learning approach with genetic and coral reefs metaheuristics for enhanced defect detection in software. International Journal of Information Management Data Insights 2022;2(2):100105. https://doi.org/10.1016/j.jjimei.2022.100105. 2022/11/01/.

[30] Yin L, Li S. Hybrid metaheuristic multi-layer reinforcement learning approach for two-level energy management strategy framework of multi-microgrid systems. Eng Appl Artif Intell 2021;104:104326. https://doi.org/10.1016/j.engappai.2021.104326. 2021/09/01/.

[31] Irshad K, Islam N, Gari AA, Algarni S, Alqahtani T, Imteyaz B. Arithmetic optimization with hybrid deep learning algorithm based solar radiation prediction model. Sustainable Energy Technologies and Assessments 2023;57:103165. https://doi.org/10.1016/j.seta.2023.103165. 2023/06/01/.

[32] Kothona D, Panapakidis IP, Christoforidis GC. Day-ahead photovoltaic power prediction based on a hybrid gradient descent and metaheuristic optimizer. Sustainable Energy Technologies and Assessments 2023;57:103309. https://doi.org/10.1016/j.seta.2023.103309. 2023/06/01/.

[33] Mishra M, Byomakesha Dash P, Nayak J, Naik B, Kumar Swain S. Deep learning and wavelet transform integrated approach for short-term solar PV power prediction. Measurement 2020;166:108250. https://doi.org/10.1016/j.measurement.2020.108250. 2020/12/15/.

[34] Mirjalili S. The Ant Lion Optimizer. Advances in Engineering Software 2015;83:80–98. https://doi.org/10.1016/j.advengsoft.2015.01.010. 2015/05/01/.

[35] Mirjalili S. Dragonfly algorithm: a new meta-heuristic optimization technique for solving single-objective, discrete, and multi-objective problems. Neural Computing and Applications 2016;27(4):1053–73. https://doi.org/10.1007/s00521-015-1920-1. journal articleMay 01,.

[36] Mirjalili S, Mirjalili SM, Lewis A. Grey Wolf Optimizer. Advances in Engineering Software 2014;69:46–61. https://doi.org/10.1016/j.advengsoft.2013.12.007. 3//.

[37] Faris H, Aljarah I, Al-Betar MA, Mirjalili S. Grey wolf optimizer: a review of recent variants and applications. *Neural Computing and Applications,* journal article 2018;30(2):413–35. https://doi.org/10.1007/s00521-017-3272-5. July 01,.

[38] Heidari AA, Mirjalili S, Faris H, Aljarah I, Mafarja M, Chen H. Harris hawks optimization: algorithm and applications. Future Generation Computer Systems 2019;97:849–72. https://doi.org/10.1016/j.future.2019.02.028. 2019/08/01/.

[39] Ghasemi M, Mohammadi Sk, Zare M, Mirjalili S, Gil M, Hemmati R. A new firefly algorithm with improved global exploration and convergence with application to engineering optimization. Decision Analytics Journal 2022;5:100125. https://doi.org/10.1016/j.dajour.2022.100125. 2022/12/01/.

[40] Rawat N, Thakur P, Singh AK, Bhatt A, Sangwan V, Manivannan A. A new grey wolf optimization-based parameter estimation technique of solar photovoltaic. Sustainable Energy Technologies and Assessments 2023;57:103240. https://doi.org/10.1016/j.seta.2023.103240. 2023/06/01/.

[41] Sulaiman MH, Mustaffa Z, Saari MM, Daniyal H. Barnacles Mating Optimizer: a new bio-inspired algorithm for solving engineering optimization problems. Eng Appl Artif Intell 2020;87:103330. https://doi.org/10.1016/j.engappai.2019.103330. 2020/01/01/.

[42] Holland JH. Genetic Algorithms. Sci. Am. 1992;267(1):66–73 [Online]. Available, http://www.jstor.org/stable/24939139.

[43] Rashedi E, Nezamabadi-pour H, Saryazdi S. GSA: a Gravitational Search Algorithm. Inf Sci (Ny) 2009;179(13):2232–48. https://doi.org/10.1016/j.ins.2009.03.004. 2009/06/13/.

[44] Eberhart R, Kennedy J. A new optimizer using particle swarm theory. In: MHS'95. Proceedings of the Sixth International Symposium on Micro Machine and Human Science; 1995. p. 39–43. https://doi.org/10.1109/MHS.1995.494215. 4-6 Oct1995.

[45] Awad H, Salim KME, Gül M. Multi-objective design of grid-tied solar photovoltaics for commercial flat rooftops using particle swarm optimization algorithm. Journal of Building Engineering 2020;28:101080. https://doi.org/10.1016/j.jobe.2019.101080. 2020/03/01/.

[46] Rao RV, Savsani VJ, Vakharia DP. Teaching–Learning-Based Optimization: an optimization method for continuous non-linear large scale problems. Inf Sci (Ny) 2012;183(1):1–15. https://doi.org/10.1016/j.ins.2011.08.006. 2012/01/15/.

[47] Lee KS, Geem ZW. A new meta-heuristic algorithm for continuous engineering optimization: harmony search theory and practice. Comput Methods Appl Mech Eng 2005;194(36):3902–33. https://doi.org/10.1016/j.cma.2004.09.007. 2005/09/23/.

[48] Ashraf WM, Uddin GM, Arafat SM, Krzywanski J, Xiaonan W. Strategic-level performance enhancement of a 660 MWe supercritical power plant and emissions reduction by AI approach. Energy Conversion and Management 2021;250:114913. https://doi.org/10.1016/j.enconman.2021.114913. 2021/12/15/.

[49] Cabello-López T, Carranza-García M, Riquelme JC, García-Gutiérrez J. Forecasting solar energy production in Spain: a comparison of univariate and multivariate models at the national level. Appl Energy 2023;350:121645. https://doi.org/10.1016/j.apenergy.2023.121645. 2023/11/15/.

[50] Ashraf WM, Dua V. Artificial intelligence driven smart operation of large industrial complexes supporting the net-zero goal: coal power plants. Digital Chemical Engineering 2023;8:100119. https://doi.org/10.1016/j.dche.2023.100119. 2023/09/01/.

[51] Shaban WM, Elbaz K, Zhou A, Shen S-L. Physics-informed deep neural network for modeling the chloride diffusion in concrete. Eng Appl Artif Intell 2023;125:106691. https://doi.org/10.1016/j.engappai.2023.106691. 2023/10/01/.

[52] Adedeji BP, Kabir G. A feedforward deep neural network for predicting the state-of-charge of lithium-ion battery in electric vehicles. Decision Analytics Journal 2023;8:100255. https://doi.org/10.1016/j.dajour.2023.100255. 2023/09/01/.

[53] Heidari M, Moattar MH, Ghaffari H. Forward propagation dropout in deep neural networks using Jensen–Shannon and random forest feature importance ranking. Neural Networks 2023;165:238–47. https://doi.org/10.1016/j.neunet.2023.05.044. 2023/08/01/.

[54] Liu X. Approximating smooth and sparse functions by deep neural networks: optimal approximation rates and saturation. J Complex 2023;79:101783. https://doi.org/10.1016/j.jco.2023.101783. 2023/12/01/.

[55] Mall PK, et al. A comprehensive review of deep neural networks for medical image processing: recent developments and future opportunities. Healthcare Analytics 2023;4:100216. https://doi.org/10.1016/j.health.2023.100216. 2023/12/01/.

[56] Wang T, Zheng X, Zhang L, Cui Z, Xu C. A graph-based interpretability method for deep neural networks. Neurocomputing 2023;555:126651. https://doi.org/10.1016/j.neucom.2023.126651. 2023/10/28/.
[57] Zheng S, Lan F, Castellani M. A competitive learning scheme for deep neural network pattern classifier training. Appl Soft Comput 2023;146:110662. https://doi.org/10.1016/j.asoc.2023.110662. 2023/10/01/.
[58] Zhong Y, Zhou J, Li P, Gong J. Dynamically evolving deep neural networks with continuous online learning. Inf Sci (Ny) 2023;646:119411. https://doi.org/10.1016/j.ins.2023.119411. 2023/10/01/.
[59] W. Muhammad Ashraf et al., "Optimization of a 660 MWe Supercritical Power Plant Performance—A Case of Industry 4.0 in the Data-Driven Operational Management Part 1. Thermal Efficiency," *Energies*, vol. 13, no. 21, https://doi.org/10.3390/en13215592.
[60] Bamisile O, et al. Deep hybrid neural net (DHN-Net) for minute-level day-ahead solar and wind power forecast in a decarbonized power system. Energy Reports 2023;9:1163–72. https://doi.org/10.1016/j.egyr.2023.05.229. 2023/10/01/.
[61] Dozono C, Inage S-i. Development of forecasting method of time variation of net solar output over wide area using grand data based neural network. Solar Compass 2023;7:100050. https://doi.org/10.1016/j.solcom.2023.100050. 2023/09/01/.
[62] Etxegarai G, López A, Aginako N, Rodríguez F. An analysis of different deep learning neural networks for intra-hour solar irradiation forecasting to compute solar photovoltaic generators' energy production. Energy for Sustainable Development 2022;68:1–17. https://doi.org/10.1016/j.esd.2022.02.002. 2022/06/01/.
[63] Keddouda A, et al. Solar photovoltaic power prediction using artificial neural network and multiple regression considering ambient and operating conditions. Energy Conversion and Management 2023;288:117186. https://doi.org/10.1016/j.enconman.2023.117186. 2023/07/15/.
[64] Mert İ. Agnostic deep neural network approach to the estimation of hydrogen production for solar-powered systems. Int J Hydrogen Energy 2021;46(9):6272–85. https://doi.org/10.1016/j.ijhydene.2020.11.161. 2021/02/03/.
[65] Sulaiman MH, Mustaffa Z, Zakaria NF, Saari MM. Using the evolutionary mating algorithm for optimizing deep learning parameters for battery state of charge estimation of electric vehicle. Energy 2023;279:128094. https://doi.org/10.1016/j.energy.2023.128094. 2023/09/15/.
[66] Sulaiman MH, Mustaffa Z, Saari MM, Daniyal H, Mirjalili S. Evolutionary mating algorithm. Neural Computing and Applications 2023;35(1):487–516. https://doi.org/10.1007/s00521-022-07761-w. 2023/01/01.
[67] Sulaiman MH, Mustaffa Z. Using the evolutionary mating algorithm for optimizing the user comfort and energy consumption in smart building. Journal of Building Engineering 2023;76:107139. https://doi.org/10.1016/j.jobe.2023.107139. 2023/10/01/.
[68] A. Kannal. *Solar Power Generation Data*. [Online]. Available: https://www.kaggle.com/datasets/anikannal/solar-power-generation-data.
[69] Storn R, Price K. Differential Evolution – A Simple and Efficient Heuristic for global Optimization over Continuous Spaces. Journal of Global Optimization 1997;11(4):341–59. https://doi.org/10.1023/A:1008202821328. 1997/12/01.
[70] S. Rubaiee and M.A. Fazal, "The Influence of Various Solar Radiations on the Efficiency of a Photovoltaic Solar Module Integrated with a Passive Cooling System," *Energies*, vol. 15, no. 24, https://doi.org/10.3390/en15249584.
[71] Ebhota WS, Tabakov PY. Influence of photovoltaic cell technologies and elevated temperature on photovoltaic system performance. Ain Shams Engineering Journal 2023;14(7):101984. https://doi.org/10.1016/j.asej.2022.101984. 2023/07/01/.
[72] Lachance J. Hardy–Weinberg Equilibrium and Random Mating. *Encyclopedia of evolutionary biology*, R. M. kliman editor. Oxford: Academic Press; 2016. p. 208–11.
[73] N.E. Benti, M.D. Chaka, and A.G. Semie, "Forecasting Renewable Energy Generation with Machine Learning and Deep Learning: current Advances and Future Prospects," *Sustainability*, vol. 15, no. 9, https://doi.org/10.3390/su15097087.